ORIGINAL PAPER

Cyclic voltammetry simulation at microelectrode arrays with COMSOL Multiphysics®

**Alessandro Lavacchi · U. Bardi · C. Borri ·
S. Caporali · A. Fossati · I. Perissi**

Abstract The present paper reports the results obtained applying the general purpose software COMSOL Multiphysics® to the finite elements simulation of Cyclic Voltammetries (CV's) at microelectrodes arrays (MEA). CV's at inlaid micro disk electrode arrays have been simulated benchmarking our results with those obtained by Compton with the finite difference method. Then the influence of meshing on the quality of the simulated data have been investigated showing that bad meshing may provide shapes with no physical meaning. Simulations have also been performed on recessed micro disk arrays in order to show the effect of the depth of the recess on the voltammetric wave shape. We found that COMSOL Multiphysics® provides a flexible and straightforward route to the simulation of electrochemical systems with complex geometry.

Keywords Cyclic voltammetry · Microelectrodes arrays (MEA's) · Finite elements · COMSOL Multiphysics®

1 Introduction

The use of microelectrode arrays (MEA's) in electrochemistry is quickly rising. Main reasons are a better signal to noise ratio and a lower capacitance compared to that of large planar electrode. Stationary voltammetric waveforms are easily obtained for CV's even at high potential scan rates. These features make MEA's an attracting choice for electroanalytical sensors [1, 2]. The theoretical determination of the electrochemical response of MEA's is not as straightforward as that of simple planar geometries for the convolution of physical and geometric effects. Only analytical approximated expressions have been derived for the prediction of stationary CV's current in the case of microelectrodes [3]. Since the optimum signal is obtained under radial diffusion conditions the simulation plays here a key role. The overlap of the diffusion clouds from neighborhood electrode may destroy the radial behavior moving progressively to linear diffusion conditions. The result is a lowering of the current density and the occurrence of peak shaped CV's. In the MEA's design such condition has to be avoided. The calculations performed in the present paper aim at assessing the use of COMSOL Multyphysics® as a tool for the simulation of CV's at MEA's. The main purpose is to provide an aid to the design of MEA's by an "a priori" analysis of the diffusion behavior of the systems as a function of microelectrodes radius and interelectrodic distances. An assessment of the method in terms of the quality of the results is provided, comparing our findings with those obtained by Compton et al. for analogous inlaid MEA's [4]. Meshing is usually critical in the finite elements especially when diffusion at edges is involved. The effect of mesh refinements with a special focus on electrode edges has been taken into account to determine the number of elements which guarantee sufficiently accurate results within the lower computation time.

More complex geometry are often encountered in MEA's. That is the case of recessed microelectrode. Here CV's can be successfully simulated with numerical methods.

A. Lavacchi (✉) · U. Bardi · C. Borri · S. Caporali ·
A. Fossati · I. Perissi
Department of Chemistry, University of Firenze,
Via della Lastruccia, 3, 50019 Sesto Fiorentino, FI, Italy
e-mail: alessandro.lavacchi@unifi.it

1.1 Equations

All the simulation performed in the paper assumed the following electrochemical reaction:

$$A + e \rightleftarrows B. \tag{1}$$

Charge balance has not been taken into account according to the supporting electrolyte hypothesis which will be discussed later. For the (1) we assumed $E_0 = 0$ V. The whole mass transport problem related to reaction (1) is described by a couple of Nernst Planck equations.

$$\frac{\partial c_i}{\partial t} + \nabla \cdot (-D_i \nabla c_i - u_i z_i F c_i \nabla \phi + c_i \vec{u}) = R_i, \tag{2}$$

where c_i is the concentration of A and B; D_i the diffusion coefficient of A and B; u_i the mobility of A and B; z_i the charge of A and B; F the Faraday's constant (96,487 °C mol^{-1}); ϕ the electric potential; $\vec{u}$ the velocity field; R_i the reaction term for A and B.

The terms due to the migration and convection are neglected here. The assumption is justified by the presence of a supporting electrolyte and the absence of convection, both common facts in dynamic electrochemistry investigations. Also the reaction term has been neglected, since no chemical reactions of the electroactive species have been assumed for the bulk of the electrolyte. Under these conditions Eq. 2 reduces to the time dependent diffusion law as described by a couple of Fick's second equations:

$$\frac{\partial c_i}{\partial t} + \nabla \cdot (-D_i \nabla c_i) = 0. \tag{3}$$

Diffusion coefficients were set to 10^{-9} m^2 s^{-1} for both A and B. The effect of the charge transfer kinetic was included in the mathematical formulation of the problem in the boundary conditions. The (1) is assumed to be a charge transfer controlled reaction, so the Butler–Volmer equation hold (4):

$$i = i_0 \left[\exp\left(\frac{\alpha_A n F}{RT} \eta\right) - \exp\left(-\frac{\alpha_C n F}{RT} \eta\right) \right], \tag{4}$$

where i_0 is the exchange current density; η the overpotential ($V - E_0$); n the number of exchanged electrons; α_A the anodic charge transfer coefficient; α_C the cathodic charge transfer coefficient; R the gas constant; T the temperature.

Equation 2 is not suitable for the use as a flux boundary condition for a mass transport problem, since it is expressed in terms of current densities. To use it in our model we need to rearrange it to Eq. 5:

$$M = C_{\text{ox}} Kf - C_{\text{red}} Kb, \tag{5}$$

where M is the mass flow density expressed as the number of moles crossing the unit surface in the time unit and Kf and Kb are given by Eqs. 6 and 7, respectively:

$$Kf = K_{\text{het}} \cdot e^{\left(\frac{\alpha_A n F \eta}{RT}\right)}, \tag{6}$$

$$Kb = K_{\text{het}} \cdot e^{\left(\frac{-\alpha_C n F \eta}{RT}\right)}. \tag{7}$$

In our simulations K_{het} was set to 10^{-2} m s^{-1}, α_A and α_C were set to 0.5 while the number of exchanged electrons n and the temperature were fixed to 1 and 298 K, respectively. All the simulations have been performed for a single CV cycle between 0.5 and -0.5 V with a scan rate of 0.1 V s^{-1}.

2 Computation

The simulation of CV's at square arrays of both inlaid and recessed microdisk have been considered here. To reduce the problem from a 3D to a 2D axial symmetry to limit the computation time, we applied the domain wall approximation described in [4–8] as shown in Fig. 1. A sketch of the cross section of the simulation cell is shown in Fig. 2a for the inlaid MEA's and Fig. 2b for the recessed MEA's. According to the domain wall approximation the relation between the inter-electrode distance d and the R_0 parameter is the following:

$$R_0 = 0.564d. \tag{8}$$

The COMSOL Nernst Plank without electroneutrality application mode has been selected. Two equations have been set to account for the transport of both A and B. Referring to Fig. 2, insulation/symmetry boundary

Fig. 1 The diffusion domain approximation for a regular array of microelectrodes with cubic geometry, as described in [4–8]
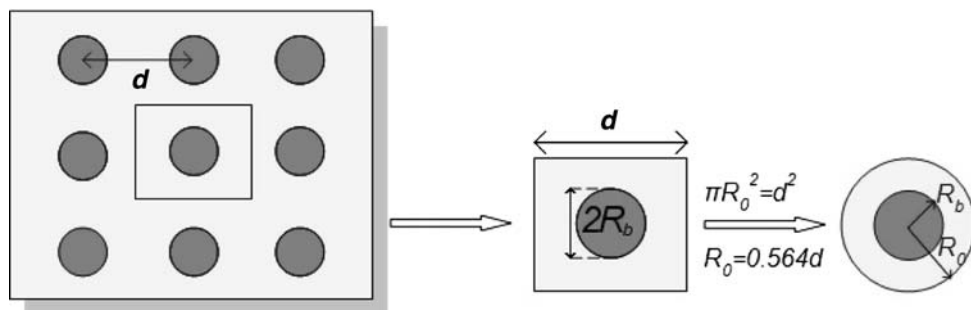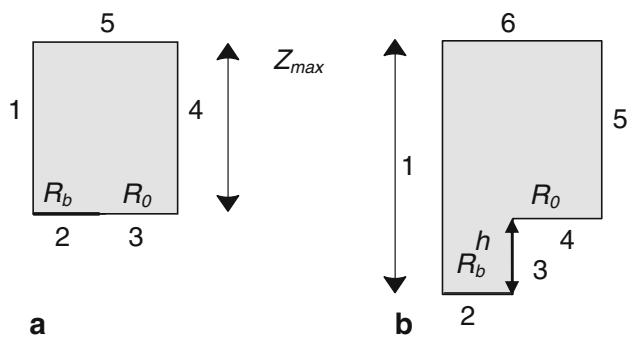
Fig. 2 Sketch of the simulation geometries: **a** inlaid and **b** recessed. Z_{max} is the height of the simulated cell and h is the recess depth

conditions have been set for boundaries 1, 3, 4, 5 for the inlaid electrode and 1, 3, 4, 5, 6 for the recessed case. Equation 5 has been set as flux boundary condition for the boundary 2 for both the inlaid and recessed microdisk. In order to avoid effects due to the finiteness of the domain, the simulation cell height was set larger than the maximum diffusion layer thickness. According to what reported in the literature [3] we defined the cell height Z_{max} as:

$$Z_{max} = \sqrt{6Dt_{max}}, \tag{9}$$

where t_{max} is the time required for the forward part of the CV scan and D is the diffusion coefficient. The domain has been meshed with Lagrange triangular quadratic elements. Triangular elements have been selected to allow local mesh refinement. The simulations of any of the presented CV's have been performed with successive mesh refinement until no appreciable changes occurred in the simulated curves. All the simulations have been carried out on a linux PC equipped with 4 Gb of ram and a 3.60 GHz Intel Pentium 4 processor. The COMSOL Multyphysics release used for the present investigation was the 3.2.

3 Results

3.1 Inlaid microdisk electrodes

Figure 3 report the results of the simulation of the CV curves at three MEA's, respectively, with R_b of 0.1, 1, and 10 μm and a R_0 fixed at 20 μm. Figure 3a shows that MEA's with 0.1 μm microelectrode provide a CV shape which is a stationary waveform. As the electrode size increases, the shape of the curves moves progressively to peak shaped CV indicating the occurrence of linear diffusion (Fig. 3b, c). The fact is explained considering that diffusion clouds overlap when the ratio between R_b and R_0 becomes larger. Such superimposition provides diffusion to propagate almost orthogonally to the electrode surface approaching the limit condition of an infinitely large planar
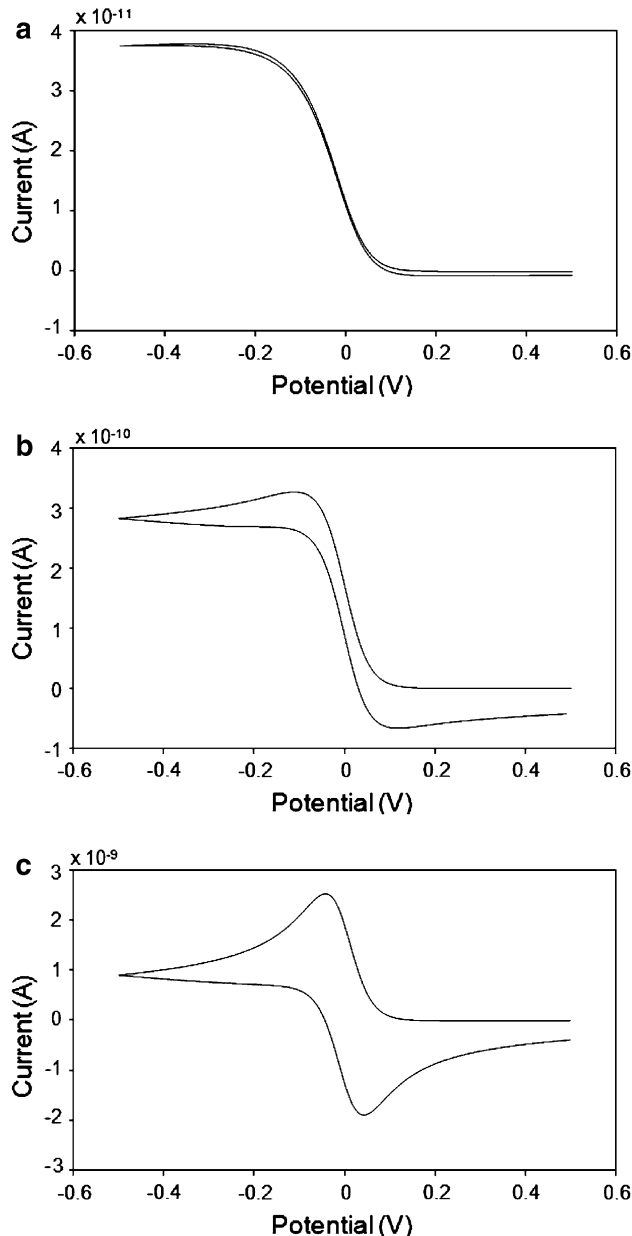

Fig. 3 Cyclic Voltammetry simulated on a microelectrode array with **a** $R_b = 0.1$ μm and $R_0 = 20$ μm, **b** $R_b = 1$ μm and $R_0 = 20$ μm and **c** $R_b = 10$ μm and $R = 20$ μm

electrode. If the R_b/R_0 ratio is small diffusion occurs in a radial way with negligible overlap.

Simulations have been performed at a constant electrode radius ($R_b = 10$ μm) and varying the distance among the electrode centers. Here we noticed that the CV is dominated by the linear diffusion for $R_0 = 20$ μm (Fig. 4a), and progressively approach to a stationary waveform when R_0 is increased to 50 (Fig. 4b) and 100 μm (Fig. 4c).

In our simulations we found that the meshing is critical especially for the smaller electrode size (0.1 μm) as expected. Bad meshing can result in curve with no physical
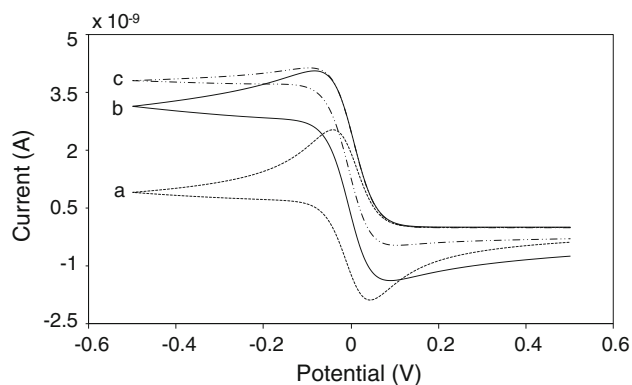
Fig. 4 Cyclic Voltammetry simulated on a microelectrode array with (a) $R_b = 10$ μm and $R_0 = 20$ μm, (b) $R_b = 10$ μm and $R_0 = 50$ μm and (c) $R_b = 10$ μm and $R_0 = 100$ μm

meaning as those showed in Fig. 5a and b. Here the current rises up even in the backward scan in the range between −0.3 and 0 V. A local mesh refinement in the electrode's region (boundary 2) is needed to correctly solve the problem. The shape of the curve in fact modifies passing from 1,027 elements, to 1,636 elements and finally to 3,951 elements (Fig. 5b, c). The latter simulation produces a correct stationary curve as reported in Fig. 5c. Further refinement of the mesh size in the boundary 2 does not provide any significant variation of the current, while increases dramatically the computation time. Table 1 lists the number of elements generated for each of the performed simulation and the computation times obtained with our configuration.

Table 2 reports the maximum current densities obtained in this investigation and those obtained by Compton et al. [4] with finite the difference method for $R_0 = 500$ μm and R_b set to 10, 1, and 0.1 μm. Results are in good agreement and demonstrate the effectiveness of the use of a multipurpose software for such simulations.

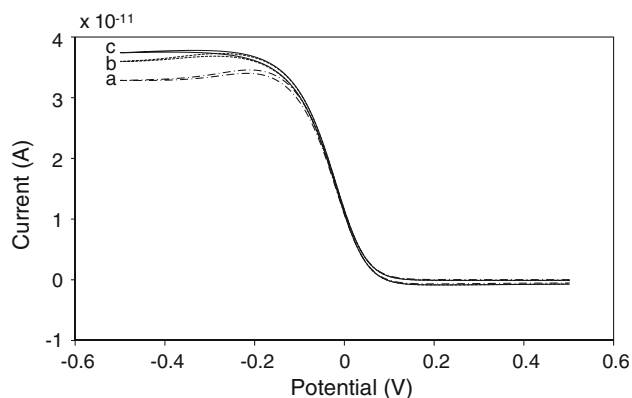**Fig. 5** Cyclic Voltammetry simulated on a microelectrode array with $R_b = 0.1$ μm and $R_0 = 20$ μm; (a) Number of elements: 1,027; (b) Number of elements: 1,636; (c) Number of elements: 3,951

3.2 Recessed microdisk electrodes

The parameter investigated here is the depth of the recess. R_0 and R_b were fixed at 10 and 100 μm, respectively. Figure 6c shows the result of the simulation of a recessed microdisk electrode with a recess depth of 10 μm. The waveform here is close to that of Fig. 4c. The reason is trivial. The depth of the recess is just 10 μm and the diffusion cloud quickly exit from it reaching the radial diffusion regime.

The situation changes a lot when the depth increases to 33 μm. The CV (Fig. 6b) is clearly peak shaped. At higher overpotential the response approaches to a stationary one. That is because the peak occurs when the diffusion cloud propagates inside the recess, but very closed to top of it. So just a few moments after reaching the peak the cloud starts to propagate in a radial way providing again a stationary answer.

Figure 6a reports the CV waveform at a recessed microdisk electrode array with recess depth of 100 μm. The voltammetric wave shows here a pronounced peak and no massive transition to radial diffusion regime occurs. During the whole simulated time the diffusion front propagates mostly inside the recess again in a linear diffusion fashion. The main difference between a CV from large planar electrodes occurs at very large overpotential. The slope of the curve here is less pronounced indicating that the contribution of the radial diffusion outside the recess is not negligible. Table 1 shows that there are not appreciable difference in the computational as a function of the depth of the recess, and that the solution times are quite in the same range of those obtained for the inlaid MEA's.
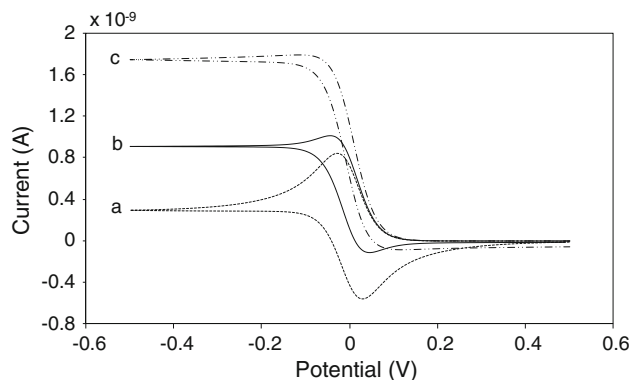
4 Conclusions

We proved that the finite element engine of COMSOL Multiphysics® can solve the equation governing diffusion complex electrochemical systems. First the method has been assessed by the simulation of systems which CV response has just been reported in the literature finding a complete agreement and stressing the importance of meshing. We found that bad meshing can lead to curve with no physical meaning. In order to get accurate results a refinement of the mesh, until no further changes in the shape of the simulated curve is observed, has to be performed. To avoid an excessive demanding of computational resources the improvement of meshing may occur trough local mesh refinement on critical points such as those representing the electrode edges. Applying such changes in the COMSOL graphic user interface is a straightforward task. We also showed that the application of the model can be extended to the simulation of even

Table 1 Time of computing for different geometries with number of mesh elements

Geometrical parameters	Number of elements	Solution time (s)
$R_b = 0.1$ μm, $R_0 = 20$ μm (Fig. 5a)	1,027	34
$R_b = 0.1$ μm, $R_0 = 20$ μm (Fig. 5b)	1,636	57
$R_b = 0.1$ μm, $R_0 = 20$ μm (Fig. 5c)	3,951	113
$R_b = 10$ μm, $R_0 = 20$ μm	13,787	445
$R_b = 10$ μm, $R_0 = 50$ μm	14,045	385
$R_b = 10$ μm, $R_0 = 100$ μm	14,271	400
$R_b = 10$ μm, $R_0 = 100$ μm, $h = 10$ μm	13,887	395
$R_b = 10$ μm, $R_0 = 100$ μm, $h = 33$ μm	13,701	420
$R_b = 10$ μm, $R_0 = 100$ μm, $h = 100$ μm	13,695	436
$R_b = 0.1$ μm, $R_0 = 500$ μm	11,344	287
$R_b = 1$ μm, $R_0 = 500$ μm	10,864	283
$R_b = 10$ μm, $R_0 = 500$ μm	10,408	287

Table 2 Comparison of the limiting currents (I_p) for some geometrical parameters with the ones obtained by Compton et al. [4]

Geometrical parameters	I_p (A)	I_p [4] (A)
$R_b = 0.1$ μm, $R_0 = 500$ μm	$3.88 \cdot 10^{-11}$	$3.89 \cdot 10^{-11}$
$R_b = 1$ μm, $R_0 = 500$ μm	$3.90 \cdot 10^{-10}$	$3.92 \cdot 10^{-10}$
$R_b = 10$ μm, $R_0 = 500$ μm	$4.23 \cdot 10^{-9}$	$4.28 \cdot 10^{-9}$

Fig. 6 Cyclic Voltammetry simulated on a recessed microelectrode array with $R_b = 10$ μm, $R_0 = 100$ μm and recess depth: (a) $h = 100$ μm; (b) $h = 33$ μm; (c) $h = 10$ μm

more complex geometries such as recessed microdisk MEA's, providing a valuable tool for the estimation of the electrochemical behavior of system which cannot be accurately described by approximated analytical solution. Here we explored the effect of the recess on the shape of the CV showing that radial or linear diffusion occurs for small (10 μm) or large (100 μm) recess depth compared to the diffusion length and finding the shape of the CV for an intermediate case (33 μm). In the end we found that COMSOL Multyphysics® is an excellent and flexible tool for the simulation of complex electrochemical systems which can easily help to explore the behavior of "real" systems. The more complex is the geometry and the larger is the advantage in using such software. Under such context a work with the main purpose of assessing the accuracy of MEA's based electroanalytical determination due to the geometric tolerances of the production process is currently under progress and will be the subject for a future publication.

References

1. Aoki K (1993) Electroanalysis 5:627
2. Arrigan DWM (2004) Analyst 129:1157
3. Britz D (2005) Digital simulations in electrochemistry. Springer, Berlin
4. Davies TJ, Compton RG (2005) J Electroanal Chem 585:63
5. Amatore C, Save'ant J-M, Tessier D (1983) J Electroanal Chem 147:39
6. Davies J, Ward-Jones S, Banks CE, del Campo J, Mas R, Muñoz FJ, Compton RG (2005) J Electroanal Chem 585:51
7. Gavaghan DJ (1996) J Electroanal Chem 420:147
8. Davies TJ, Banks CE, Compton RG (2005) J Solid State Electrochem 9:797